A Miniature Short Stroke Tubular Linear Actuator and its Control

Haiwei Lu, Jianguo Zhu, Youguang Guo, and Zhiwei Lin
Center for Electric Machines and Power Electronics, Faculty of Engineering
University of Technology, Sydney
Australia

***Abstract*— Miniature actuators are the critical components in the robotic applications with high intelligence, high mobility and small scales. Among various types of actuators, linear actuators show advantages in many aspects. A miniature short stroke PM tubular linear actuator for the micro robotic applications is presented in this paper. The actuator is deliberately designed based on the optimal force capability and a proper sensorless control scheme is developed for the driving of the actuator. Experiment both on the prototype of the actuator and the drive system show the validity of the design.**

Keywords—tunbular linear actuator; sensorless control; micro robotics

I. INTRODUCTION

Robotics in future may be with high intelligence and mobility but in a much smaller package. Miniature actuators are therefore the critical components to make these machines more dexterous, compact and cost effective. In general, actuators can be divided into two main types according to their motion behavior: rotary and linear. For a system that requires linear motion, linear actuators show advantages in terms of efficiency, thrust control, and system volume [1]. Particularly, linear actuators can greatly simplify the drive mechanisms, which is crucial to the compactness of the systems. Moreover, application of powerful permanent magnet (PM) materials and advanced control strategies can result in higher force-to-volume ratio, better performance, and less cost of the machines. Among various linear machine configurations, PM tubular machines excitation have a number of distinctive features, such as high force density and excellent servo characteristics, which make them an attractive candidate for those applications in which dynamic performance and reliability are critical [2].

This paper presents a newly developed short stroke PM tubular linear actuator which aims to the miniature robotic applications. In order to acquire good force capability, the actuator is deliberately designed based on the magnetic field analysis. Prototype of the actuator was constructed to verify the design. Due to the limited space in the miniature application, the physical position sensors are not permitted for the drive control of the designed actuator, and hence a sensorless drive scheme is designed for the actuator. Simulation and experiment show the satisfactory performance of the actuation system.

II. SHORT STROKE TUBULAR LINEAR ACTUATOR

A. Basic Structure

The overall size of the proposed short stroke tubular linear PM actuator is according to the typical size of a medical capsule. The actuator was designed with an external diameter of 6.4mm and the total length is approximately 12mm. Fig.1 shows the basic configuration of the actuator and the elementary dimensions of the actuator are listed in Table I. The tubular stator core and pole-pieces on translator are made up of the glassy metal film, which is an amorphous soft magnetic material with high magnetic permeability and extremely low core loss. Circular concentrated three-phase windings are mounted inside the stator core. Due to small diameter of the actuator, the slotless winding structure is employed for the simplicity in construction and better performance.

The translator of the actuator is constructed by stacking the disc-shape NdFeB magnets and pole-pieces alternately along a non-ferromagnetic shaft, as shown in Fig.1. The use of non-ferromagnetic shaft can reduce the effective air gap between the stator and translator. Two caps are attached at each side of the stator core acting as the supporter and guide way for the translator. The caps are also made up of nonmagnetic material to reduce the fringing flux as well as the mass of the actuator.

B. The Number of poles

The number of poles is one of the most important parameters that can greatly affect the machine configuration and performances. In the linear actuator design, the amount of the magnets is determined based on the tradeoff between the flux density and the saturation of the magnetic core.

According to the study conducted in [4], as the number of poles is increased, the saturation in the magnetic core

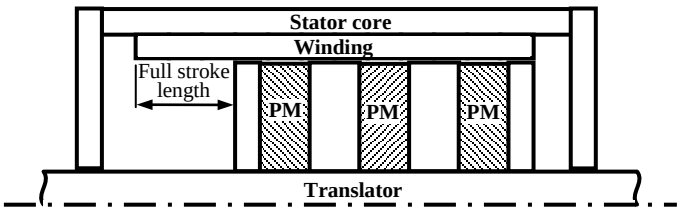

Fig.1 Basic configuration

Table I
MAJOR DIMENSIONS OF THE ACTUATOR

Dimensions	Symbol
Outer diameter of stator core	D_e
Inner diameter of stator core	D_o
Thickness of stator core	tc_{ex}
Length of stator core	l_s
Diameter of translator	D_a
Length of translator	l_m
Diameter of translator shaft	D_s
Pole pitch	τ
Thickness of pole-pieces	τ_c
Thickness of magnets	τ_m
Height of magnets	h_m
Height of the stator winding	h_c
Air gap	g

diminishes and the reluctance will decrease, resulting in higher air gap flux densities and higher force production of the actuator. Although multi-pole configuration requires the current flow direction to match the polarities of the magnets, electronic commutation with/without position sensor can be used. However, a pole number more than four will not contribute much to the force production but reduces the available stroke of the actuator.

For the proposed interior mounted linear actuator, a three-magnet topology was applied by considering the length of machine stator core, attainable stroke length and the available thickness of NdFeB magnet. The configuration can result in a high air gap flux and a good acceleration-per-ampere-turns ratio.

C. Design for Maximum Force Capability

Because the force of an electromagnetic actuator will decrease dramatically due to the scaling effect [5], much concern should be taken on the force performance when designing the miniature actuator. It can be derived that the electromagnetic force of the linear actuator, F_{em}, is given by

$$F_{em} = 2p\phi_p J_s h_c, \tag{1}$$

where ϕ_p is the magnetic flux under one pole, J_s the current density in the stator windings, h_c the height of the stator windings, and p the number of poles. Through an analytical analysis of the magnetic field, it can be found that the flux per pole can have a maximum value when τ_m equals half of the pole pitch τ if keeping other dimension as constants [5]. Accordingly, to obtain a maximum magnetic flux per pole, the magnets and pole-pieces should be designed with the same thickness.

In addition to the thickness of the magnet, the height of the magnet h_m also affects the attainable force of the actuator. By further magnetic field analysis one can yield following relationship,

$$F_{em} = 2\mu_0 \pi p H_c J_s \frac{\tau^2 k_m (1-k_m)(k_s+k_m)(1+k_s+k_m) G_H}{16 k_m (1-k_m)(k_s+k_m) G_H + \tau^2 (1+k_s+k_m)}, \tag{2}$$

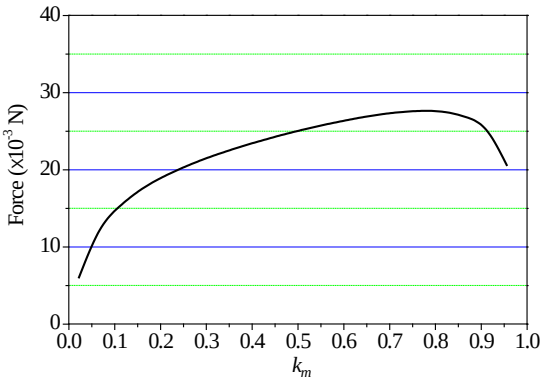

Fig.2 Variation of force vs. k_m obtained by analytical analysis

where G_H is the gap between the stator core and translator shaft, $k_m=h_m/G_H$ the magnetic occupation ratio, and $k_s=D_s/G_H$. If the dimensions of the stator and translator shaft are defined, G_H and k_s will be constants and F_{em} varies with k_m and τ. As previously discussed, the pole pitch has been determined by the selection of the thickness of magnet. Hence, the variation of force versus k_m can be drawn out and the result is illustrated in Fig.2.

From the above results, it can be seen that there also exists an optimal values of k_m that can make the electromagnetic force achieve its maximum value, and it can be found by applying $dF_{em}/dk_m = 0$ to (2). However, it should be noted that there is no universal solution that can be derived from (2) for actuators with various pole pitches and the result can only applies to certain design.

D. Prediction of Actuator Performance

Based on the design conducted above, the performance of the designed linear actuator was analyzed. Because the actuator has a symmetric structure, a 2D FE model with axisymmetric element property is established to analyze the magnetic performance of the actuator.

Different force characteristics of the actuator can be obtained by various excitation schemes. In applications of PM electric machines, conventional three-phase AC sinusoidal excitation and 2-phase DC excitation are the commonly used driving method. Hence, the electromagnetic forces under the both methods are examined.

For the 3-phase sinusoidal excitation, the excitation currents in three phases are set as follows

$$\begin{cases} I_a = \sqrt{2} I_0 \sin\left((\pi/\tau)\cdot x_{sm} - \pi/3\right) \\ I_b = \sqrt{2} I_0 \sin\left((\pi/\tau)\cdot x_{sm} + \pi/3\right), \\ I_c = \sqrt{2} I_0 \sin\left((\pi/\tau)\cdot x_{sm} - \pi\right) \end{cases} \tag{3}$$

where x_{sm} is the translator position with respect to the stator windings, and I_0 the *rms* value of the phase current. By using this translator position based current setting, one can achieve a maximum attainable force provided by the actuator, known as field-oriented control method that is commonly used in the

servo control of rotary PM machines. Fig.3 shows the computed force under excitation of 3-phase sinusoidal currents. Maximum force can be achieved when the translator is in the middle of the stator windings, which is around 29mN. The salient effect caused by the translator structure is visible throughout the force curve. The force reduces when the translator is close to the extremities of the actuator due to the fringing effect of the magnetic field. When the translator is at the ends of the stator windings, the attained force will drop down to about 26mN, about 10% less compared to the maximum attainable force.

The 2-phase DC excitation, generally known as the brushless DC drive method, are widely used in the PM brushless machine drives due to its simple implementation and very good control performance. Moreover, the brushless DC drives without the mechanical position sensors can also be easily realised by phase voltage detection technique. These features are attractive for the micro systems that do not allow complex system structure and large volume.

A proper switching sequence for the 2-phase DC excitation can be found by comparing the produced forces under different conduction schemes and Table II shows the obtained switching sequence. By applying the sequence, the generated force was computed and the result is shown in Fig.4. The maximum force is about 23mN. Due to the DC phase currents interacting with sinusoidal magnetic field as well as the current commutations, there are large ripples in the produced force when driven by 2-phase DC excitation. The force ripples can be up to 20% with an average force of 21mN.

TABLE II
SWITCHING SEQUENCE FOR 2-PHASE EXCITATION

Stroke	0 – 13.3%	13.3 – 50%	50 – 86.7%	86.7 – 100%
Energization Sequence	$\overline{AB}$	$\overline{BC}$	$\overline{AC}$	$\overline{AB}$

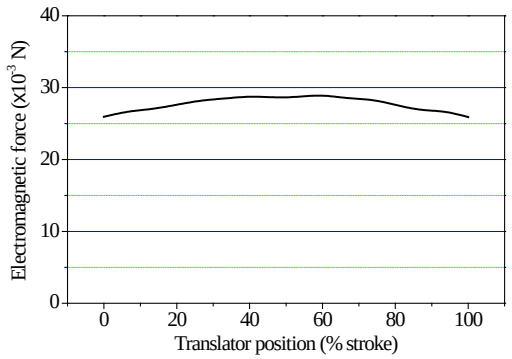

Fig.3 Electromagnetic force under sinusoidal excitation

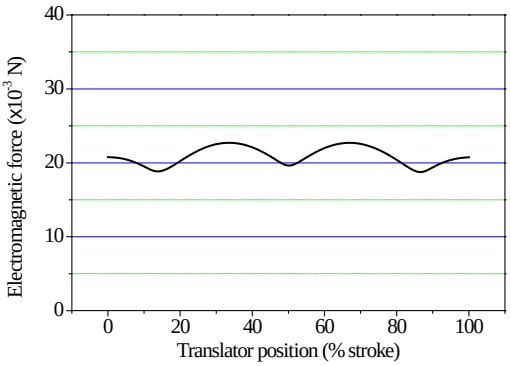

Fig.4 Electromagnetic force under 2-phase DC excitation

III. PROTOTYPE CONSTRUCTION AND TEST

The proposed actuator contains many miniature components with high precision requirements and the conventional methods such as punching, nibbling, acid etching or conventional electrical discharge machining (EDM) are no longer able to meet the machining demands. Instead, the precision laser machining technology is employed for the fabrication of the key components of the actuator, such as the stator core and pole pieces. Fig.5 (a) and (b) show the fabricated stator core with windings and the stacked translator, and Fig.5(c) shows the completed prototype of the linear actuator.

A test bench is specially designed for testing the prototypes. The schematic diagram of the test bench is illustrated in Fig.6. It consists of a force gauge, a micro position meter, a tool set used for clamping the actuator, and a supporting stage with a screw. The position of the actuator's translator can be preset by the micrometer before the testing. The force gauge is attached to a sliding block mounted on a screw so that it can move accurately by turning the screw. The combination of the micro meter and the force gauge can be used for clamping the translator at a certain position with a preload exerted by the force gauge. As a result, the performance measurements of the actuator, such as the phase inductances and actuation forces, can be performed at any desired translator positions.

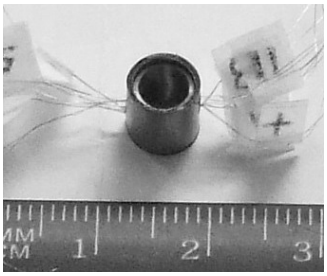

(a) Stator and windings

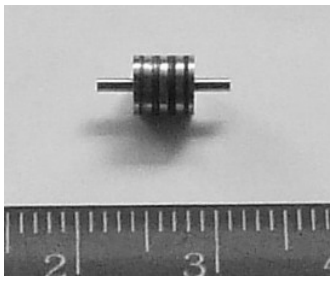

(b) Translator

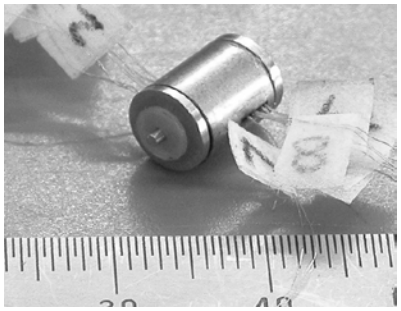

(c) Completed prototype

Fig.5 Fabrication of the linear actuator

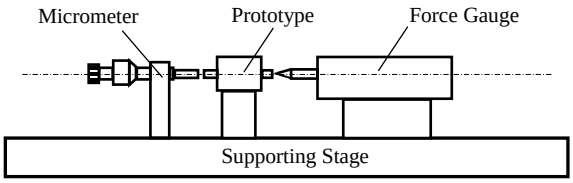

Fig.6 Schematic diagram of the test bench

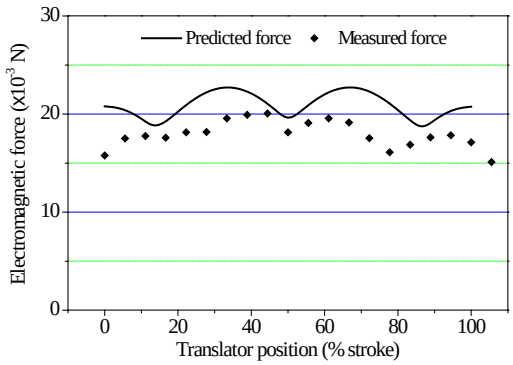

Fig.7 Actuation force of the prototype

By using the test bench, the force of the actuator under 2-phase DC excitation was measured as the actuator would be driven by the brushless DC scheme in its control system design. During the measurement, a phase current in accordance with that in the performance prediction was applied to the actuator. Fig.7 shows the measured forces and the predicted results are also plotted for comparison. It can be seen that the measured results agree well with the predicted forces and this shows the validity of the design.

IV. Control of the Tubular Linear Actuator

The proposed tubular linear actuator is in fact a type of three-phase brushless PM synchronous machine and it can be operated either as a brushless AC machine or a brushless DC machine. As previously mentioned, the brushless DC drive method would be preferable for the designed actuator because of its simple implementation, compact structure, which are essential for the micro applications, and this makes the brushless DC drive method the first choice for the controller design of the proposed actuator.

The measurement of rotor position is crucial for the operation of brushless PM machine. However, there is usually no spare room for the installation of any type of linear mechanical position sensor within the restricted micro robotic systems. A sensorless control scheme must be employed for the control of the actuator.

A. Machine Modelling for the Control Design

In order to evaluate and verify the control performance of the actuator, an accurate machine model is essential. Considering the operation of the actuator under brushless DC drive scheme, a proper dynamic model incorporating the electronic commutation and power electronics must be considered.

Regarding the switching sequence in the brushless DC drive, there are three combinations of phase connections caused by the switching of the solid-state switches: *A-B*, *B-C* and *C-A*. The formulation of the actuator model is then derived according to these connection patterns as

$$R_j i_j + L_{jj}\frac{di_j}{dt} + L_{jk}\frac{di_k}{dt} = u_j - e_j - u_n , \quad (4)$$

$$R_k i_k + L_{kk}\frac{di_k}{dt} + L_{kj}\frac{di_j}{dt} = u_k - e_k - u_n , \quad (5)$$

$$\frac{di_k}{dt} + \frac{di_j}{dt} = 0 , \quad (6)$$

$$i_j + i_k = 0 , \quad (7)$$

where R and L are the phase resistance, inductance and current, u, i, and e the phase voltage, current and back EMF, u_n is the neutral voltage, and subscripts j and k denote the energized phases determined by the switching sequence. By solving the above equations, the electrical dynamic performance of the actuator can be obtained.

A SIMULINK model of the designed actuator was developed based on the above analysis, as illustrated in Fig.8. The model contains two blocks: the electrical block and the mechanical block. Both blocks are implemented by applying the state equations of the actuator in the S-functions provided by SIMULINK. The electrical block calculates the phase currents, back EMFs and electromagnetic force of the actuator based on the input phase voltages. The mechanical block incorporates the kinetic model of the actuator to find out the velocity and displacement of the translator by using the input electromagnetic force and load force. The mechanical block can also be further reconfigured according to the different kinetic properties when the actuator is applied to various mechanical systems.

B. Sensorless Control of the Linear Actuator

Basically, two types of sensorless control technique for brushless PM machines can be found in the literature. The first type is the position sensing technique using the back EMF, and the second is the position estimation using the machine parameters, terminal voltages, and currents [6]. The second

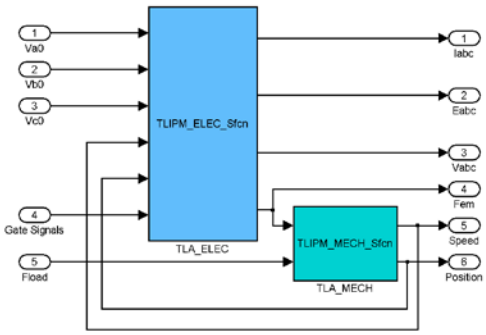

Fig.8 SIMULINK model of the actuator

scheme usually needs high performance micro processors such as digital signal processors (DSPs) to implement the complicated algorithm of rotor position estimation, and the cost of the system is relatively high. On the other hand, the back EMF sensing scheme is much simple and can be easily realized by less hardware implementation. This feature is therefore preferred for the compact systems, especially micro systems. However, the back EMF sensing scheme can only be employed in brushless DC drive (2-phase excitation) as it relies on detecting the back EMF in the unexcited phase of the machine.

Considering the micro application of the designed linear actuator, the back EMF sensing scheme is adopted due its simple implementation and effectiveness. It is also possible to implement the entire control system onto one single chip device and be integrated with the actuator so as to make the actuator and control system a compact device.

Through the magnetic field analysis, the magnetizing flux density in each phase can be found, as shown in Fig.9. According to the sensorless brushless DC drive principle, it can be seen that there are three commutation positions during the entire stroke of the translator, i.e. P1, P2 and P3 shown in the figure. If the translator is starting from zero position, the commutation positions P2 and P3 can be determined by the detection of zero crossing points (ZCPs) in the back EMFs of phase *A* and phase *B*, which are ZCP1 and ZCP2. If the translator is operating in opposite direction, the commutation positions P2 and P1 can be also determined by detecting these ZCPs.

However, only two ZCPs throughout the entire stroke make it difficult to find the first commutation point during the operation because there is no ZCP taken place before the corresponding commutation no matter which side the translator is started from. To overcome this problem, one of the methods is to integrate the back EMF of the unexcited phase [7].

Since the back EMF in each phase is proportional to the corresponding magnetizing flux density shown in Fig.9, for a certain traveling distance, the integration of the back EMF $\int edt$ will be constant despite the traveling speed of the translator. Based on this principle, the integration of the back EMF in the unexcited phase can be used to determine the desired commutation operation. However, this method is highly machine-dependant since the designed flux density is distinct from machines to machines. The integration threshold can only be appropriately set based on a good understanding of the magnetic characteristics of the machine.

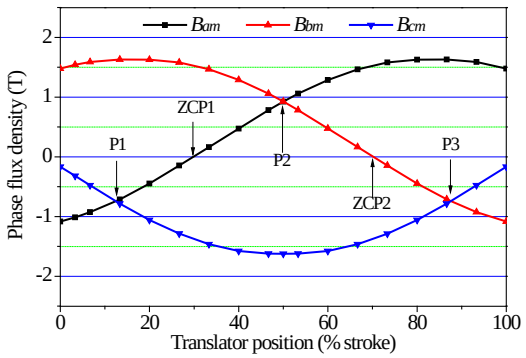

Fig.9 The magnetizing flux density in each phase

C. *Performance Simulation*

In order to evaluate the performance of the designed actuation system, the developed control algorithm for the linear actuator was implemented in SIMULINK. Together with the developed model of the actuator, the performance of the actuator with the developed sensorless control scheme was simulated and analyzed. Fig.10 shows the SIMULINK model of the sensorless drive system of the actuator.

The driving performance of the actuator with no load is firstly simulated. Fig.11 shows the back EMF of each phase and the generated ZCP detection signals. By using these ZCP detection signals, the phase currents commutate effectively during the operation. As a result, the transition of the

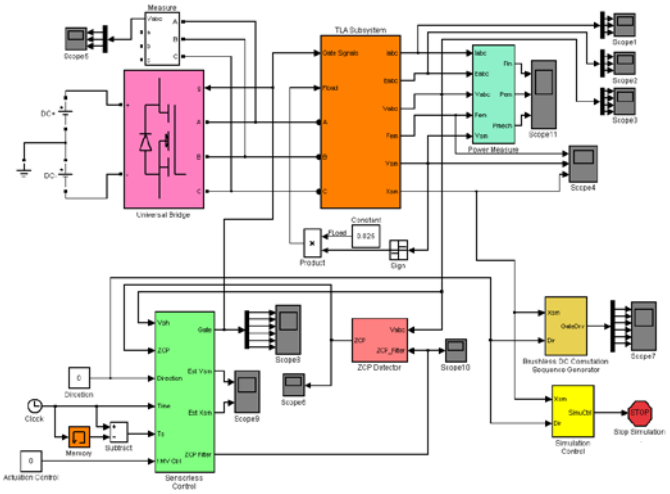

Fig.10 SIMULINK model of the sensorless control system for the linear actuator

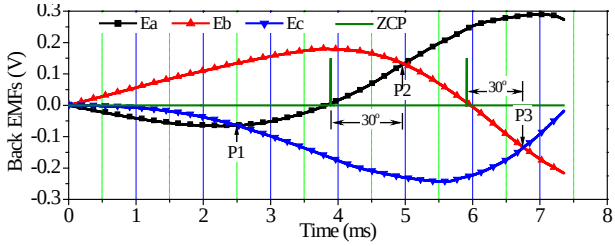

Fig.11 Back EMFs and ZCP signals

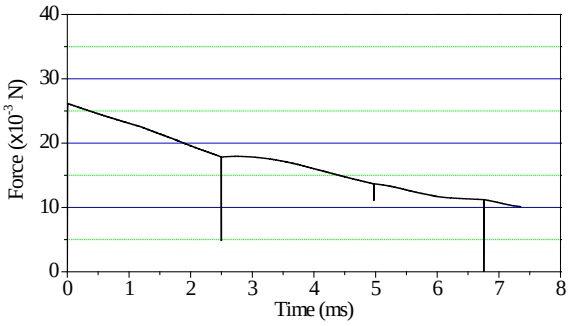

Fig.12 Actuation force of the linear actuator with no load

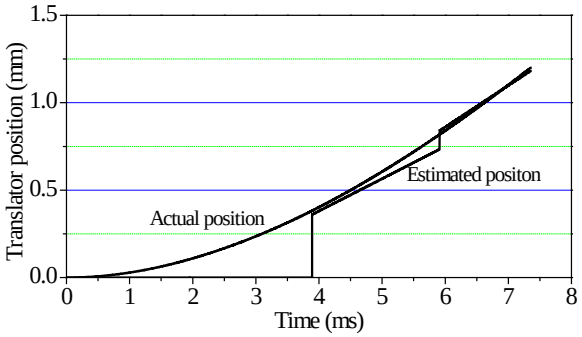

Fig.13 Actual and estimated translator positions

electromagnetic force of the actuator is appropriate and smooth, as shown in Fig.12. Fig.13 shows the translator position with respect to the stator and the estimated values by the control algorithm are much closed to the actual positions.

V. EXPERIMENTAL VERIFICATION

The experiment of actuation control system was based on the dSPACE DS1104 prototyping system. The block diagram for the control experiment of the actuator is illustrated in Fig.14. Besides of the microprocessor board provided by the DS1104 system, a driving board was developed including the power converter and signal sensing system. With the dSPACE real-time interface, the control algorithm developed in the SIMULINK environment was directly put into practice by using the controller hardware and the corresponding software.

There was no external load applied to the actuator during the experiment and the frictional force between the translator and stator played as the load. The results showed that the commutation of the electronic converter was accurately carried out as in the performance simulation and the thrust control of the actuator was effectively implemented in both directions. Fig.15 plots the translator position with respect to the stator estimated by the control algorithm during the positive direction experiment and it was similar to that obtained from the performance simulation. The maximum speed of the translator during the operation could be up to 0.26m/s.

VI. CONCLUSION

A short stroke tubular PM linear actuator was developed for linear motion micro robotic systems. Within the desired overall dimensions, the actuator was deliberately designed to acquire optimum force capability and it was verified by testing on a fabricated prototype. Due to the limited space in the miniature application, a sensorless drive scheme is developed for the driving control of the actuator. Through the dynamic modeling of both the actuator and control system, the actuation performance was examined and the results showed the validity

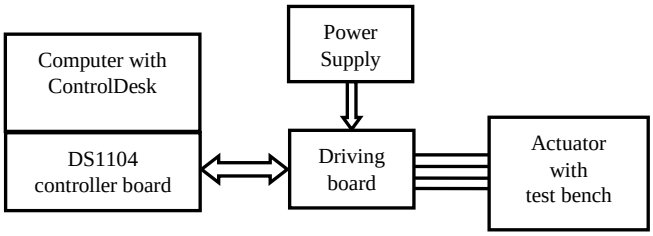

Fig.14 Block diagram of the experimental system

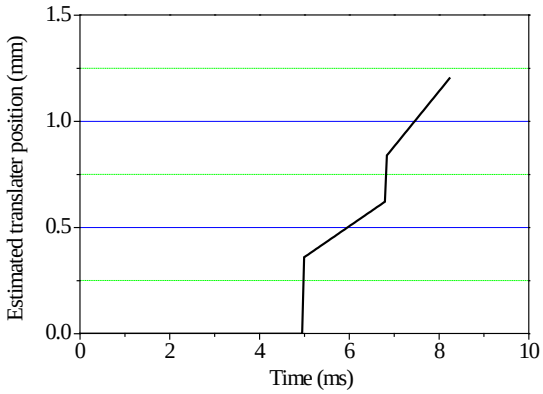

Fig.15 Estimated translator position during the operation

and effectiveness of the design. The actuation experiment carried out on the developed actuator control system demonstrated the satisfactory operational performance and the system could be used for the locomotion of micro robotics.

REFERENCES

[1] N. Bianchi, S. Bolognani, and F. Tonel, "Design consideration for a tubular linear PM servo motor," *EPE Journal*, vol.11, no.3, pp. 41-47, Aug. 2001.

[2] Jiabin Wang, G. W. Jewell, and D. Howe, "A general framework for the analysis and design of tubular linear permanent magnet machines," *IEEE Trans. Magn.*, vol. 35, no. 3, pp.1986-2000, May 1999.

[3] B. Lequesne, "Permanent magnet linear motors for short strokes," *IEEE Trans. Ind. Applicat.*, vol. 32, pp.161-168, Jan.-Feb.1996.

[4] Haiwei Lu and Jianguo Zhu; "A comparative study of microactuators driven by electric and magnetic principles," in *Proc. Australasian Universities Power Engineering Conference*, ID. 79, Sept. 2004.

[5] Haiwei Lu, Jianguo Zhu, and Youguang Guo, "Development of a slotless tubular linear interior permanent magnet micro motor for robotic applications," *IEEE Trans. Magn.*, vol. 41, no. 10, pp. 3988-3990, Oct. 2005.

[6] J. W. Shao, *Direct Back EMF Detection Method for Sensorless Brushless DC (BLDC) Motor Drives*, Master Thesis, Virginia Polytechnic Institute and the State University, USA, 2003.

[7] T. M. Jahns, R. C. Becerra, and M. Ehsani, "Integrated current regulation for a brushless ECM drive," *IEEE Trans. Power Electron.*, vol. 6, no. 1, pp. 118-126, Jan. 1991.